surface-wave filter applications. The results indicate, however, that the presence of the electrodes cannot be neglected even at low frequencies where the electrode thickness is negligible compared to the acoustic wavelength. The results further suggest that at high frequencies, where the mass of the electrodes might affect the surface-wave velocity, similar phase-compensating electrodes would be required even in low coupling materials.

References

[1] R. H. Tancrell, M. B. Schultz, H. H. Barrett, L. Davis, Jr., and M. G. Holland, "Dispersive delay lines using ultrasonic surface waves," *Proc. IEEE* (*Special Issue on Topside Sounding and the Ionosphere*) (Lett.), vol. 57, pp. 1211–1213, June 1969.
[2] L. R. Adkins, W. L. Bongianni, P. J. Hagon, and A. J. Hughes, "Microwave magnetic and acoustic materials, microwave surface wave techniques," ECOM, Ft. Monmouth, N. J., Final Rep. ECOM-0321-F, Dec. 1970.
[3] C. C. Tseng, "Elastic surface waves on free surface and metallized surface of CdS, ZnO and PZT-4," *J. Appl. Phys.*, vol. 38, p. 4281, 1967.
[4] J. J. Campbell and W. R. Jones, "A method for estimating optimal crystal cuts and propagation directions for excitation of piezoelectric surface waves," *IEEE Trans. Sonics Ultrason.*, vol. SU-15, pp. 209–217, Oct. 1968.
[5] W. R. Smith, H. M. Gerard, J. H. Collins, T. M. Reeder, and H. J. Shaw, "Analysis of interdigital surface wave transducers by use of an equivalent circuit model," *IEEE Trans. Microwave Theory Tech.* (*Special Issue on Microwave Acoustics*), vol. MTT-17, pp. 856–864, Nov. 1969.
[6] K. A. Ingebrigtsen, "Surface waves in piezoelectrics," *J. Appl. Phys.*, vol. 40, pp. 2681–2686, 1969.
[7] B. A. Richardson and G. S. Kino, "Probing of elastic surface waves in piezoelectric media," *Appl. Phys. Lett.*, vol. 16, pp. 82–84, 1970.

An Accurate Junction Circulator Design Procedure

STEVEN J. SALAY AND HARRY J. PEPPIATT

Abstract—**A two-step design procedure for the accurate synthesis of a junction circulator is given. The procedure is accurate to within a few decibels for isolation in the 20- to 40-dB range.**

The theory of the stripline junction circulator [1], [2] has been useful to the designer in a qualitative way, but it falls short of predicting the broad-band performance required in many applications. Bosma [3] has proposed a broad-band circulator model involving three coupled gyrators connected as shown in Fig. 1. Z_{cir} is the impedance related to the resonant modes coupled by the gyrators and the gyrator impedance, as indicated. For the stripline junction circulator, Bosma [3] has obtained the following relation for Z_{cir}:

$$\frac{1}{Z_{\mathrm{cir}}} = 0.67\eta\left[\frac{\sqrt{3}(\kappa/\mu)}{x} - j\frac{J_1'(x)}{J_1(x)}\right]$$

$$x = \frac{2\pi R}{\lambda_0}\sqrt{\epsilon\mu_e}$$

$$\eta = 4\pi\frac{R}{W}\sqrt{\frac{\epsilon_0\epsilon}{\mu_0\mu_e}}\,\frac{1}{\ln\left[(W+D)/(W+T)\right]} \tag{1}$$

where

- $J_1(x), J_1'(x)$ first-order Bessel function and its derivative,
- μ_e effective permeability,
- ϵ dielectric constant of ferrite,
- R radius of ferrite pucks,
- W, D, T width, height, and thickness of the stripline coupled to the pucks.

A more general result applicable to microstrip and other line couplings is obtained by replacing η by η' where

$$\eta' = \frac{\pi R}{W Z_0}\sqrt{\frac{\epsilon}{\epsilon_d \mu_e}} \tag{2}$$

Manuscript received April 26, 1971; revised July 23, 1971. This correspondence is part of S. J. Salay's dissertation submitted to the Virginia Polytechnic Institute and State University, Blacksburg, Va., in partial fulfillment of the requirements for the Ph.D. degree.
The authors are with the Telecommunication Products Department, General Electric Company, Lynchburg, Va. 24502.

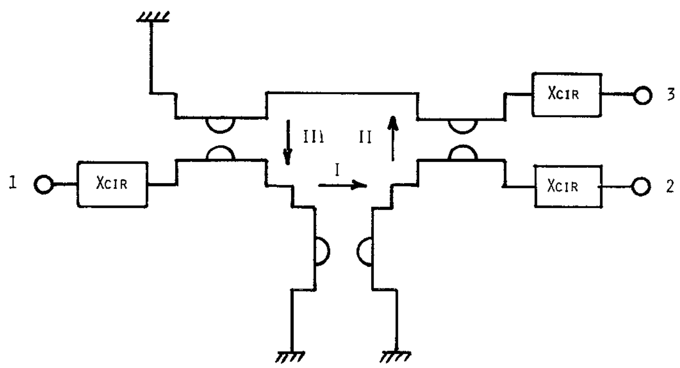

Fig. 1. Circulator model proposed by Bosma. X_{cir} is the imaginary part of Z_{cir}. The real part of Z_{cir} is the gyrator impedance of each gyrator.

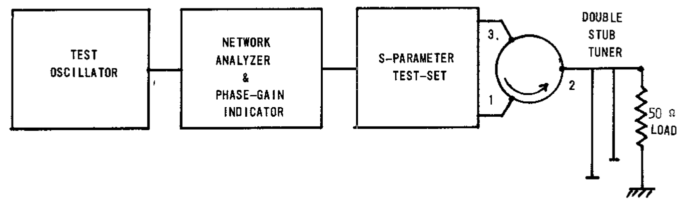

Fig. 2. Block diagram of the measuring setup for determining Z_{cir}.

and

- ϵ_d effective dielectric constant of the line,
- Z_0 the characteristic impedance of the line.

Bosma [3] and others [5] have indicated that the circuit of Fig. 1 gives only qualitative agreement with measured performance, especially for below resonance circulators. This correspondence is an attempt to show that the model itself is quite accurate and that discrepancies arise due to the inaccuracy in the boundary value solution for Z_{cir}. Also, a two-step design procedure for accurate circulator synthesis is given.

It is easily shown (Fig. 1) that if the complex conjugate of Z_{cir} is used as the load at port 2, ideal isolation is obtained between the driven port, port 1, and port 3. In this condition, the input impedance at port 1 is Z_{cir}. With an experimental setup[1] shown in Fig. 2 a point-by-point measurement of Z_{cir} versus frequency can be made by first adjusting the double stub tuner for maximum isolation at each frequency. Since Z_{cir} is the input impedance at the outer radius of the ferrite pucks, and from (2), one would suspect Z_{cir} to be dependent on line dimensions; the measurement should be made for a few different line couplings. The results of such measurements are shown in Fig. 3. The tuning stubs were adjusted to give isolation (port 1 to 3) of greater than 40 dB at each frequency in this octave bandwidth. Note that the measured change in Z_{cir} with the line dimension W is perhaps less than expected, a fact which facilitates the design procedure.

The experimental measurement of Z_{cir} is then used in a computer analysis program [5] (based on the model) which computes forward loss, return loss, and isolation. Arbitrary networks can be inserted at each port for matching purposes. With this program, one can optimize the performance to the specifications required.

A comparison of the computed and measured isolation of a circulator is shown as an example in Fig. 4. The measured circulator (a compact design using a dielectric ring) was fabricated directly from the data supplied by the computer program without any fine tuning. The agreement is within the accuracy associated with S parameter and time domain reflectometer equipment used in normal transmission line impedance measurements.

[1] This setup is similar to that used by Simon [4].

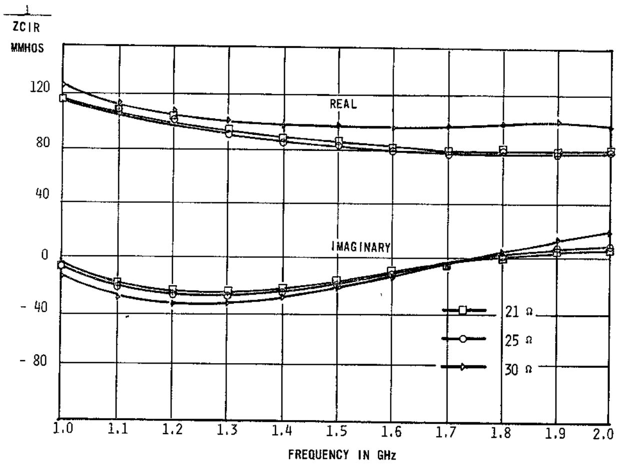

Fig. 3. Measured Z_{cir} for ferrite puck biased below resonance using different line couplings.

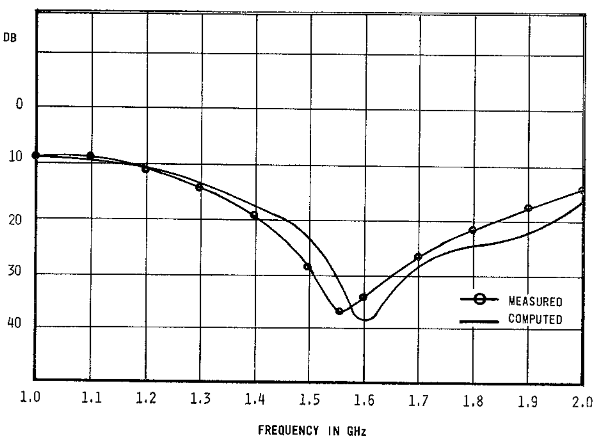

Fig. 4. Computed and measured isolation of stripline circulator.

Besides providing an accurate circulator synthesis technique, this procedure should give a means of more direct evaluation of theoretical boundary value solutions for junction circulators.

References

[1] H. Bosma, "On strip line Y-circulation at UHF," *IEEE Trans. Microwave Theory Tech.*, vol. MTT-12, pp. 61–72, Jan. 1964.
[2] C. E. Fay and R. L. Comstock, "Operation of the ferrite junction circulator," *IEEE Trans. Microwave Theory Tech.*, vol. MTT-13, pp. 15–27, Jan. 1965.
[3] H. Bosma, "A general model for junction circulators, Choice of magnetization and bias field," *IEEE Trans. Magn.*, vol. MAG-4, pp. 587–596, Sept. 1968.
[4] J. W. Simon, "Broadband strip-transmission line Y-junction circulators," *IEEE Trans. Microwave Theory Tech.*, vol. MTT-13, pp. 335–345, May 1965.
[5] S. J. Salay and H. J. Peppiatt, "Input impedance behavior of stripline circulator," *IEEE Trans. Microwave Theory Tech.* (Corresp.), vol. MTT-19, pp. 109–110, Jan. 1971.

A Compact Subsidiary-Resonance Limiter

JAMES L. ALLEN

***Abstract*—A compact subsidiary-resonance limiter with a dynamic range of greater than 200 kW is described. The structure consists of a multilayer ferrite–dielectric "sandwich" placed on the narrow wall of a reduced-height reduced-width rectangular waveguide. Below-the-threshold insertion loss is less than 0.5 dB over the 5.4–5.9-GHz band, and the threshold level is about 20 W.**

Manuscript received May 17, 1971; revised August 16, 1971. This work was supported by Sperry Microwave Electronics Division, Sperry Rand Corporation, Clearwater, Fla.
The author is with the Department of Electrical Engineering, Colorado State University, Fort Collins, Colo. 80521.

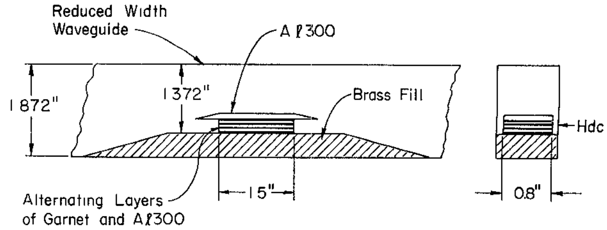

Fig. 1. Cross section of a multilayer limiter. The thicknesses of the layers, beginning with the garnet layer adjacent to the brass fill, are 0.030, 0.050, 0.030, 0.030, 0.070, 0.030, 0.030, and 0.125 in, respectively.

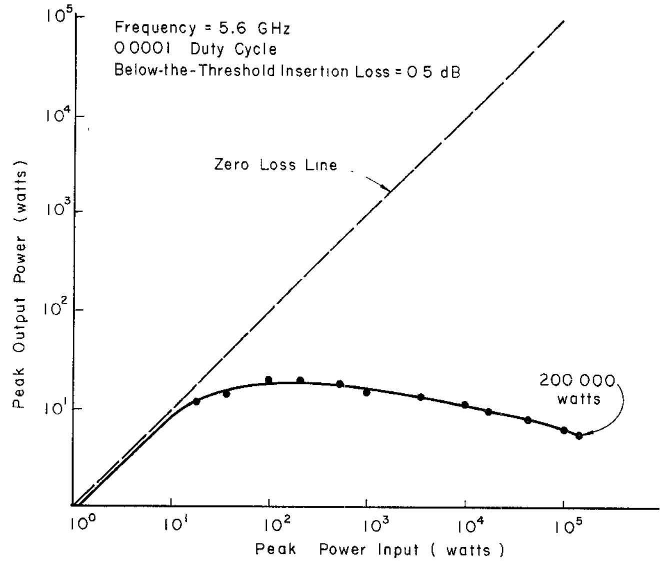

Fig. 2. High-power characteristics for the multilayer subsidiary-resonance limiter.

Subsidiary-resonance limiters have been studied extensively [1]–[4] for application in duplexing circuits. A recent paper by Carter *et al.* [5] describes a laminar limiter structure consisting of a cascade of rectangular rods of ferrite and dielectric along the narrow wall of a rectangular waveguide. The laminar structure has the distinct advantage that its threshold power level can be very low (2.8 W). The dynamic range of the laminar limiter is controlled by the number (and size) of the ferrite rods. Dynamic range of a conventional single-slab type of limiter is controlled by the length of the ferrite slab. In both cases obtaining wide dynamic range necessarily requires a relatively large structure with a long magnet. The purpose of this correspondence is to describe a multilayer loading technique that permits a wide dynamic range and a low threshold to be obtained with a physically small structure and a short magnet.

Cross-sectional views of a typical multilayer limiter structure are given in Fig. 1. This structure consists of four slabs of YIG interleaved with four slabs of Al-300 dielectric placed on the narrow wall of a reduced-height reduced-width rectangular waveguide. The ferrite and dielectric slabs are of various thicknesses selected experimentally to obtain maximum dynamic range. The ferrite slabs are only $1\frac{1}{2}$ in long. Thicknesses and other pertinent data are provided in the diagram. This multilayer limiter has a below-the-threshold insertion loss of less than 0.5 dB in the 5.4–5.9-GHz frequency band. The threshold power level is about 20 W and the dynamic range is greater than 200 kW. Characteristics of the limiter were essentially constant over the frequency range of the magnetron, 5.4–5.9 GHz. A plot of output versus input power is given in Fig. 2. Notice that the limit of the dynamic range has not been reached at a peak power input of 200 kW, which was the maximum power available from the magnetron. The finite excitation time of the nonlinear effect permits the leading edge of the input pulse to "leak through" essentially unattenuated. This is referred to as the spike leakage and its amplitude very nearly follows the zero loss line shown in Fig. 2. The width of the leakage spike